A Statistical Model for Shadowed Body-Centric Communications Channels: Theory and Validation

Simon L. Cotton, *Member, IEEE*

***Abstract*—This paper presents a new statistical signal reception model for shadowed body-centric communications channels. In this model, the potential clustering of multipath components is considered alongside the presence of elective dominant signal components. As typically occurs in body-centric communications channels, the dominant or line-of-sight (LOS) components are shadowed by body matter situated in the path trajectory. This situation may be further exacerbated due to physiological and biomechanical movements of the body. In the proposed model, the resultant dominant component which is formed by the phasor addition of these leading contributions is assumed to follow a lognormal distribution. A wide range of measured and simulated shadowed body-centric channels considering on-body, off-body and body-to-body communications are used to validate the model. During the course of the validation experiments, it was found that, even for environments devoid of multipath or specular reflections generated by the local surroundings, a noticeable resultant dominant component can still exist in body-centric channels where the user's body shadows the direct LOS signal path between the transmitter and the receiver.**

***Index Terms*—Body-centric communications, channel modeling, lognormal shadowed κ–μ distribution.**

I. Introduction

With the advent of body-centric communications, the issue of signal shadowing caused by the human body has once again been brought to the forefront [1]–[5]. Unlike the earlier studies of Obyashi and Zander [6], which considered shadowing for fixed indoor links, i.e., shadowing brought about by the intersection of the human body with the direct line-of-sight (LOS) signal path, in body-centric systems at least one end of the wireless link will be bodyworn. Dependent upon the body-centric application, e.g., on-body [7]–[9], off-body [2], [5] or body-to-body [3], [4], [10], the wireless link may be subject to continuous random shadowing of the dominant signal (including free-space LOS or strong specular) components.

Manuscript received May 08, 2013; revised September 01, 2013; accepted October 06, 2013. Date of publication December 18, 2013; date of current version February 27, 2014. This work was supported by the U.K. Royal Academy of Engineering and the Engineering and Physical Research Council (EPSRC)under Grant EP/H044191/1 and by the Leverhulme Trust, U.K., through a Philip Leverhulme Prize.

The author is with the Institute of Electronics, Communications and Information Technology, Queen's University Belfast, Belfast BT3 9DT, U.K. (e-mail: simon.cotton@qub.ac.uk).

Color versions of one or more of the figures in this paper are available online at http://ieeexplore.ieee.org.

Digital Object Identifier 10.1109/TAP.2013.2295211

For on-body channels, shadowing caused by body parts obstructing the direct link between antennas can cause substantial attenuation of the received signal. In [11], a significant body shadowing component was clearly identified in dynamic on-body channel measurements made at 2.45 GHz, while in [12], for simulations also conducted at 2.45 GHz, the differing size and (dielectric) constitution of the arm, leg, and torso was found to have a variable effect upon the shadowing region established on the opposite side of the body to the transmitter. The problem of body shadowing is particularly prevalent for millimeter-wave on-body communications at 60 GHz [13], where it is postulated that the significant shadowing effect from the human body is expected to make non-line-of-sight (NLOS) communications very difficult, if not impossible.

In off-body channels, although one end of the communications link is not worn, shadowing by the human body will still be an important factor, especially in low multipath environments. For example, in [5], it was observed that for a chest-worn patch antenna the received signal dropped by 50 dB when the user's body turned to obstruct the main LOS path even at a very short separation distances of 1 m. Body-to-body channels will, therefore, be particularly vulnerable to shadowing as they can suffer from dual node shadowing were both persons' bodies obstruct the main signal path causing the link to be lost altogether even at very short separation distances of a few meters [14].

Clearly, shadowing caused by the human body can have a considerable effect upon the communications channel. Therefore, to engineer robust hardware such as antennas and transceiver circuitry, optimize protocols and localization schemes [15] to be used in body-centric communications, its impact should be included in statistical models used to describe signal reception. Drawing inspiration from the unlikely source of land mobile satellite communications, where fading channels are known to exist in which the dominant signal component may be subject to shadow fading [16], [17], a new model for shadowed body-centric communications channels is derived.

In this model, clusters of multipath waves are assumed to have scattered waves with identical powers, alongside the presence of elective dominant signal components—a scenario which is identical to that observed in κ–μ fading [18]. The κ–μ distribution is a very general fading model which contains as special cases other important distributions such as the one-sided Gaussian, Rice (Nakagami-n), Nakagami-m, and Rayleigh distributions. While the model proposed here inherits all of this generality, the critical difference between this model and that of κ–μ fading is that the *resultant* dominant component, formed by phasor addition of the individual dominant components, is

assumed to be random. In particular, it is assumed that this resultant dominant component follows a lognormal distribution.

The contribution of this paper is threefold. First, to the best of author's knowledge, it presents a highly novel shadowed fading model for the three main types of channel encountered in body-centric communications. The new model is characterized in two formats, initially in terms of the clustered scatter and resultant dominant components, and then parameterized using the popular κ and μ parameters. This model is currently unprecedented in the literature and, due to its very general nature, it will undoubtedly find application well beyond the scope of its intended use for body-centric communications. Second and most important, it provides a thorough empirical validation of the proposed model by comparing its probability density function (pdf) with data obtained from a wide range of experiments which used considerably different experimental setups. Last, the utility of the new formulations is further demonstrated through the simulation of the received signal using the acceptance–rejection method [19].

The remainder of this paper is organized as follows. In Section II, a discussion of the different propagation phenomena encountered in body-centric communications is presented. The complex signal model proposed for shadowed body-centric communications channels is introduced in Section III. An expression for the pdf of the received signal in this shadowed fading model is also derived in Section III. For convenience, this pdf is also reparameterized into a second format, expressed in terms of κ and μ. Section IV persists with the original format of the model and provides an empirical validation for a range of body-centric channels in which shadowing of the dominant components is known to play an important role. The utility of the proposed shadowed fading model is illustrated through the fitting of the new pdf to experimental data alongside simulated data. Finally, Section V finishes the paper with some concluding remarks.

II. Shadowing in Body-Centric Communications Channels: A Discussion

Due to the dynamic nature of body-centric communications, signal transmission will often be subject to random shadowing events. This is caused by the transmitted electromagnetic waves impinging upon nonhomogenous obstacles, including body matter, which obscure the direct LOS signal path. If we initially exclude the effects of multipath generated by the local environment, in body-centric communications channels where no direct LOS path exists, the wireless link will be maintained by a number of dominant components, including diffracted and creeping (trapped surface) waves [20]. As these dominant components travel from the transmitter to the receiver, they will also form multipath clusters due to signal components being reflected and scattered by the complicated geometrical and dielectric properties of the body [21]. In reverberant environments such as inside of buildings with a high metallic content, additional multipath clusters can also be created which contribute to and in some cases dominate signal reception in body-centric channels [21].

In on-body channels such as those found in body area networks (BANs), shadowing of wireless nodes situated on the body will be largely due to the obstruction of the direct signal path by human tissue and moving limbs. For example, consider the scenario depicted in Fig. 1(a), where we have an on-body channel which spans the front-left-waist to the right-wrist positions. As the person moves their right arm from the rest position at the side of the body to the front, and then to the back of the body, the wireless link between the nodes will be subject to quasi-periodic shadowing caused by the wrist moving from the field of view of the front-left-waist node into the shadow region at the side and posterior of the body. When the arm moves to its position of maximum displacement behind the body, the wireless link will be supported by diffracted, surface, reflected, and scattered waves, which may take more than one propagation path around the body. The received signal here will be further supplemented by environmental multipath if it is present.

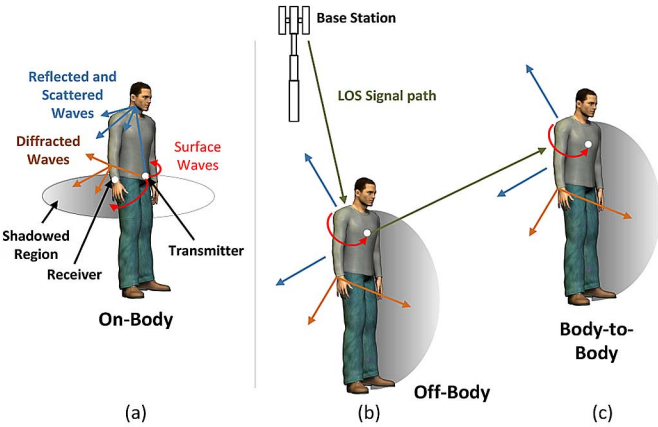

Fig. 1. Examples of scenarios where shadowing may be encountered in (a) on-body, (b) off-body, and (c) body-to-body communications channels.

Off-body communications, between a body-worn device and a transceiver in a different physical location, typically use free-space propagation to communicate. Wireless links in these applications will be particularly susceptible to frequent signal blocking events caused not only by the user's body, but also people and obstacles in the local vicinity. As shown in Fig. 1(b), the human body can substantially shadow or completely obscure the dominant signal path between the bodyworn antenna and the non-bodyworn transceiver. Similar to on-body communications, the link in this instance will be maintained by diffracted waves propagating around the body and signal scattered from the body and local surroundings. As well as suffering from the same shadowing issues as off-body communications, body-to-body systems [Fig. 1(c)] will also suffer from dual node mobility as both ends of the link will be either bodyworn or carried by the user. This may include dual-body shadowing events, when the users are orientated such that their bodies obstruct the main LOS path.

III. A Statistical Model for Shadowing in Body-Centric Communications Channels

Before beginning the derivation, it is worth reinforcing one of the main aims of this study which was to develop a statistical model that is capable of simultaneously capturing the shadowing and multipath fading observed in body-centric communications channels. In this respect, the model proposed in the rest

of the paper is a single model—that is a channel which is characterized by a single statistical distribution [17]. This is advantageous for body-centric channel modeling as not only is it well suited to the characterization of on-body channels in which separation distances between antennas do not change significantly, but it also provides a statistical description of the local shadowing and multipath fading effects for off-body and body-to-body channels when extracted from the large-scale signal fluctuation traditionally associated with mobile communications [22].

Given the physical propagation phenomena discussed in Section II, it seems plausible to assume that the received signal in body-centric communications channels is due to the same propagation mechanisms as that encountered in κ–μ fading [18], except in this instance, the resultant dominant component, which is formed by the phasor addition of the LOS components in the channel, is a random variable. In the following, it is assumed that the shadowing of the resultant dominant component in body-centric channels varies according to a lognormal distribution. In the proposed model, the complex received signal envelope $R\exp(j\theta)$ may be written as the sum of the resultant scattered waves (W) and the resultant dominant component (Δ) such that

$$R\exp(j\theta) = W\exp(j\phi) + \Delta\exp(j\phi_0) \tag{1}$$

where W follows an unknown distribution that will be determined shortly and Δ is assumed to be lognormal distributed. In this model, ϕ_0 is the phase of the resultant dominant component and ϕ is the stationary random phase process associated with W distributed over the range $[-\pi, \pi)$.

If Δ is initially held constant, then the conditional pdf of R is given by

$$f_{R|\Delta}(r|\delta) = \frac{r^{\mu}}{\sigma^2\delta^{\mu-1}}\exp\left(-\frac{r^2+\delta^2}{2\sigma^2}\right) I_{\mu-1}\left(\frac{\delta r}{\sigma^2}\right) \tag{2}$$

which is that of the κ–μ distribution [18] parameterized in terms of δ, σ, and μ, and $I_{\nu}(\bullet)$ is the modified Bessel function of the order ν. Here κ is related to δ, σ, and μ through the relationship $\kappa = \delta^2/2\mu\sigma^2$, which is simply the ratio of the total power of the dominant components (δ^2) to the total power of the scattered waves $(2\mu\sigma^2)$, $\mu > 0$ is related to the multipath clustering, and the mean power is given by

$$E\left[R^2\right] = \Omega = \delta^2 + 2\mu\sigma^2. \tag{3}$$

To determine the distribution of W, we let $\delta \to 0$ and note that for small arguments of the Bessel function [23, eq. (9.6.7)]

$$I_{\nu-1}(z) \approx \frac{\left(\frac{z}{2}\right)^{\nu-1}}{\Gamma(\nu)} \tag{4}$$

substituting this result into (2) and after some mathematical manipulation gives

$$f_{R|\Delta}(r|\delta) = \frac{r^{2\mu-1}}{2^{2\mu-1}\sigma^{2\mu}\Gamma(\mu)}\exp\left(-\frac{r^2+\delta^2}{2\sigma^2}\right). \tag{5}$$

When $\delta = 0$, the power is concentrated only in the scattered waves, and the received signal in (1) is due only to W and, thus, in this case, the conditional probability density of R becomes equivalent to that of W, which is

$$f_W(w) = \frac{w^{2\mu-1}}{2^{2\mu-1}\sigma^{2\mu}\Gamma(\mu)}\exp\left(-\frac{w^2}{2\sigma^2}\right). \tag{6}$$

By using (3) in (6) and again letting δ equal zero, it can be shown that the equation above is in fact equivalent to the Nakagami-m distribution given by

$$f_W(w) = \frac{2\mu^{\mu}}{\Omega^{\mu}\Gamma(\mu)}w^{2\mu-1}\exp\left(\frac{-\mu w^2}{\Omega}\right) \tag{7}$$

where μ is equal to the Nakagami-m parameter. To determine the distribution of R when Δ varies according to the lognormal distribution, we now calculate the conditional mathematical expectation $\int_0^{\infty} f_{R|\Delta}(r|\delta)\, f_{\Delta}(\delta)\, d\delta$, which gives

$$f_R(r) = \frac{r^{\mu}}{\sigma^2}\int_0^{\infty}\frac{1}{\delta^{\mu-1}} \times \exp\left(-\frac{r^2+\delta^2}{2\sigma^2}\right) I_{\mu-1}\left(\frac{\delta r}{\sigma^2}\right) f_{\Delta}(\delta)\, d\delta \tag{8}$$

where

$$f_{\Delta}(\delta) = \frac{1}{\delta\beta\sqrt{2\pi}}\exp\left[-\frac{(\ln\delta-\alpha)^2}{2\beta^2}\right]. \tag{9}$$

Here α and β are the location and scale parameters, respectively. Substituting (9) into (8) gives

$$f_R(r) = \frac{r^{\mu}}{\beta\sqrt{2\pi}\sigma^2} \times\int_0^{\infty}\frac{1}{\delta^{\mu}}\exp\left[-\frac{\sigma^2(\ln\delta-\alpha)^2+\beta^2(r^2+\delta^2)}{2\beta^2\sigma^2}\right] I_{\mu-1}\left(\frac{\delta r}{\sigma^2}\right)d\delta. \tag{10}$$

Equation (10) is the pdf for the shadowed fading observed in body-centric communications channels based on the model proposed here. It is a new result, which also generalizes Loo's statistical model for land mobile satellite communications channels derived in [16]. This can be obtained from (10) by setting $\mu = 1$. Unfortunately, no closed-form expression exists for (10), and the integral must be evaluated numerically. However, this can be achieved quite straightforwardly in most mathematical software packages, for example, using the `trapz` function available in MATLAB. Fig. 2 shows the shape of the new shadowed fading (NSF) pdf for a range of increasing values of μ from 0.5 to 14.5. The averaged model parameters for $\alpha = 0.5$, $\beta = 1.26$, and $\sigma = 0.5$ given in [16] are used here so that the new model can be directly compared with Loo's model.

Although (10) will be considered for the modeling of the shadowed body-centric channels studied in this paper, for completeness, it is also worth considering the parameterization of (10) in terms of κ, that is the lognormal shadowed κ–μ pdf. Assuming that the variation of the resultant dominant component δ follows (9), it is possible to perform a transformation of variables to find the distribution of κ. Once again, using the relationship $\kappa = \delta^2/2\mu\sigma^2$[18] along with (3), it follows that

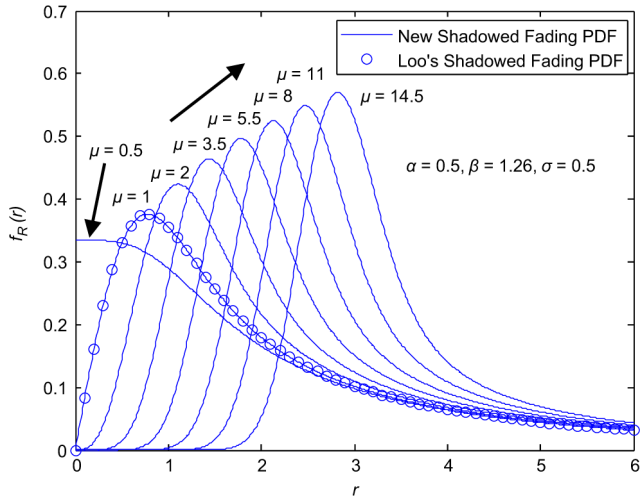

Fig. 2. NSF pdf of (10) for increasing values of μ.

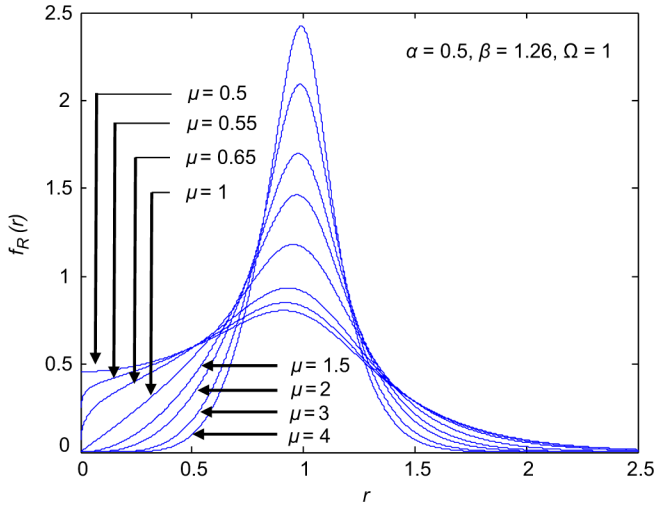

Fig. 3. Lognormal shadowed κ–μ pdf of (12) for increasing values of μ.

$\delta^2 = \kappa(1+\kappa)\Omega/2$. To obtain the pdf of the transformed variable κ, we must evaluate

$$f_{\mathrm{K}}(\kappa) = f_{\Delta}\left(\sqrt{\kappa(1+\kappa)\frac{\Omega}{2}}\right)\left|\frac{d\delta}{d\kappa}\right|$$

which, in turn, gives

$$f_{\mathrm{K}}(\kappa) = \frac{1+2\kappa}{2\beta\sqrt{2\pi\kappa(1+\kappa)}} \times \exp\left[-\frac{\left(\ln\sqrt{\kappa(1+k)\frac{\Omega}{2}} - \alpha\right)^2}{2\beta^2}\right]. \quad (11)$$

Finally, to obtain (10) parameterized in terms of κ, we must calculate the conditional mathematical expectation $\int_0^{\infty} f_{R|\mathrm{K}}(r|\kappa) f_{\mathrm{K}}(\kappa)\, d\kappa$, where $f_{R|\mathrm{K}}(r|\kappa)$ is the κ–μ distribution [18, eq. (11)]. The pdf of the received signal in κ–μ fading channels in which the resultant dominant component undergoes lognormal fading is subsequently given in

$$f_R(r) = \frac{\mu}{\beta\sqrt{2\pi\Omega}}\left(\frac{r}{\sqrt{\Omega}}\right)^{\mu}\int_0^{\infty}\frac{(1+2\kappa)(1+\kappa)^{(\mu-1)/2}}{\kappa^{(\mu+1)/2}\exp(\mu\kappa)} \times \exp\left[-\frac{\left(\ln\sqrt{\kappa(1+\kappa)\frac{\Omega}{2}} - \alpha\right)^2}{2\beta^2} - \mu(1+\kappa)\left(\frac{r}{\sqrt{\Omega}}\right)^2\right] \times I_{\mu-1}\left(2\mu\sqrt{\kappa(1+\kappa)}\left(\frac{r}{\sqrt{\Omega}}\right)\right) d\kappa. \quad (12)$$

Fig. 3 shows the shape of (12) for a range of different values of μ.

IV. Validation

A validation of the NSF pdf is now presented for body-centric communications applications. A selection of antenna positions deemed to be most susceptible to shadowing were chosen from a wide range of on-body, off-body, and body-to-body communications channels. It should be noted that, unless otherwise stated, all of the measurements conducted here were performed either in an anechoic chamber or a low multipath (outdoor) environment. These low multipath environments were chosen due their unique characteristics which allow human body effects on signal propagation to be isolated by minimizing environmental multipath contributions. As well as showing the excellent fit to empirical data, the utility of the proposed model is further demonstrated by using (10) as a foundation for acceptance–rejection-based simulation of the received signal for a selection of the body-centric channels [19].

A. On-Body

To illustrate the usefulness of the new model for characterizing shadowing in on-body channels, three links were chosen from the study performed in [24], namely, the front-left-waist to the right-head, right-knee, and right-wrist, as shown in Fig. 4(a). The measurements were conducted at 2.45 GHz in the anechoic chamber facilities at Queen's University Belfast, Belfast, U.K. The chamber had a floor area of 54 m^2 and was housed in conductive shielding and lined with pyramidal radio-frequency (RF) absorbers. The antennas used in this study were compact (5-mm height) higher mode microstrip patch antennas [20] designed specifically for on-body networking applications. The test subject was an adult male of height 1.82 m and mass 90 kg. In the experiments, the antennas were mounted so that the radiating patch element was parallel to the body surface. They were then connected to port 1 and 2 of a Rhode & Schwarz ZVB-8 vector network analyzer (VNA) using calibrated low-loss coaxial cables. The VNA was configured with an output power of 0 dBm and set to record measurements of S_{21} at 5-ms intervals for 30 s. For all of the measurements presented here, the user performed a walking motion at a set location at the center of a walkway on the right-hand side of the anechoic chamber.

Fig. 5 shows a 5-s segment of the normalized received signal envelopes for each of the three on-body channels. The quasi-periodic pattern of the received waveforms caused by the movement (and associated shadowing) of the human body is clearly

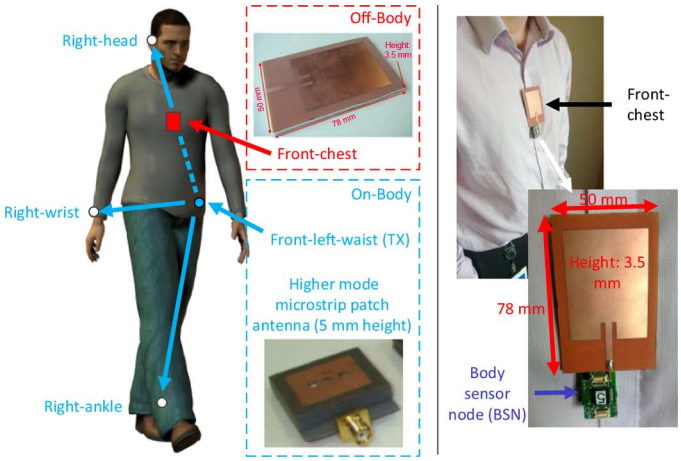

(a) (b)

Fig. 4. (a) Illustration showing antenna positions for on-body Section IV-A and off-body Section IV-B measurements; and (b) modified BSN node used for body-to-body measurements (Section IV-C).

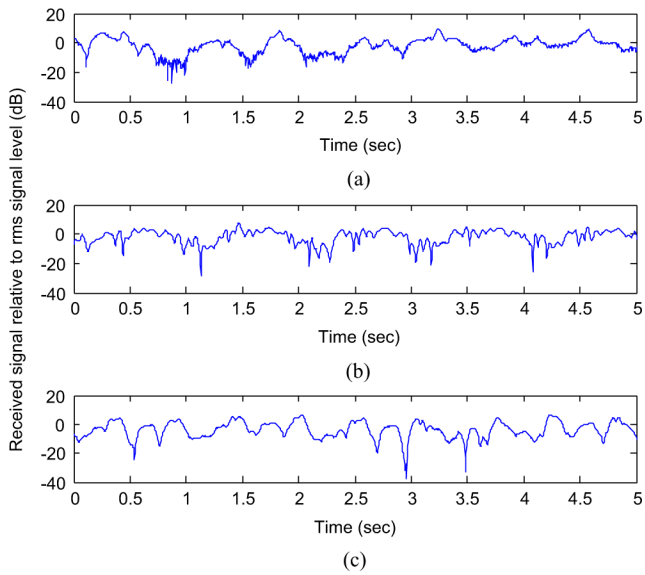

Fig. 5. Normalized received signal envelope for the front-left-waist to (a) right-head, (b) right-knee, and (c) right-wrist on-body channels.

evident. Fig. 6 shows the NSF pdf fitted to the empirical pdf for each of the three channels. For convenience, the root mean square (rms) signal level $\hat{r} = \sqrt{E[R^2]}$ is removed from the fading envelopes to enable a direct comparison of the fading characteristics for each of the on-body links. All parameter estimates for the new pdf were obtained using a nonlinear optimization algorithm in MATLAB and are given in Table I. As we can see, the NSF pdf proposed here provides an excellent fit to the measured data confirming the validity of the model when applied to on-body communications channels. Also shown inset in Fig. 6 is the distribution of the resultant dominant component for each of the three links plotted using (9). As we can see, the resultant dominant component for the front-left-waist to the right-head and right-knee positions show similar shadowing characteristics. As expected, the front-left-waist to right-wrist channel recorded the greatest spread of the resultant dominant component caused by a shadowing process due to the repetitive movement of the arm from the front to the back of the body, as depicted in Fig. 1(a).

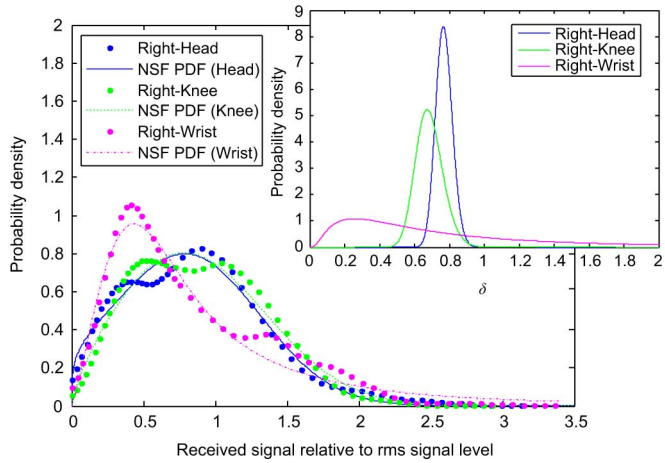

Fig. 6. NSF pdf fitted to the empirical pdf for each of the three on-body channels in the anechoic chamber. Shown inset is the estimated distribution of the shadowed resultant dominant component for each of the three links.

TABLE I
ESTIMATED PARAMETERS FOR ON-BODY CHANNELS USING NSF PDF

Anechoic Chamber					
Position	$\hat{\mu}$	$\hat{\sigma}$	$\hat{\alpha}$	$\hat{\beta}$	$\hat{r}$ (mV)
Right-Head	0.64	0.51	-0.26	0.12	0.31
Right-Knee	0.88	0.58	-0.38	0.11	1.74
Right-Wrist	1.10	0.24	-0.50	0.93	1.54
Reverberation Chamber					
Position	$\hat{\mu}$	$\hat{\sigma}$	$\hat{\alpha}$	$\hat{\beta}$	$\hat{r}$ (mV)
Right-Head	0.87	0.56	-0.36	0.09	12.17
Right-Knee	1.25	0.30	-0.32	0.50	13.86
Right-Wrist	0.77	0.33	-0.31	0.51	11.83

Fig. 7 shows the front-left-waist to right-wrist on-body link considered in isolation to highlight improvement achieved by using the new shadowed pdf for on-body channels compared to the κ–μ pdf. Here the normalized κ–μ pdf [18, eq. (1)] is used, given by

$$f_P(\rho) = \frac{2\mu(1+\kappa)^{(\mu+1)/2}}{\kappa^{(\mu-1)/2}\exp(\mu\kappa)}\rho^{\mu} \times \exp\left(-\mu(1+\kappa)\rho^2\right) I_{\mu-1}\left(2\mu\sqrt{\kappa(1+\kappa)}\rho\right) \quad (13)$$

where $P = R/\hat{r}$ Also shown in Fig. 7 is the simulated output for the front-left-waist to right-wrist on-body channel obtained using (10) with the acceptance–rejection method[1] described in [19]. As anticipated, the simulated and theoretical pdfs are virtually indistinguishable from one another.

Before concluding this section, to test the performance of the model for high multipath environments, Fig. 8 shows the measured and predicted pdfs for the same on-body channels, except this time the measurements were taken in a reverberation chamber. As we can clearly see, the proposed model still provides an exceptional fit to the data. Most interestingly though, the parameter estimates for the channels in the reverberation chamber suggest that a shadowed dominant component still persists, even though for this extreme environment, multipath was expected to dominate.

[1]The hat function used for the acceptance–rejection method was the Gamma pdf.

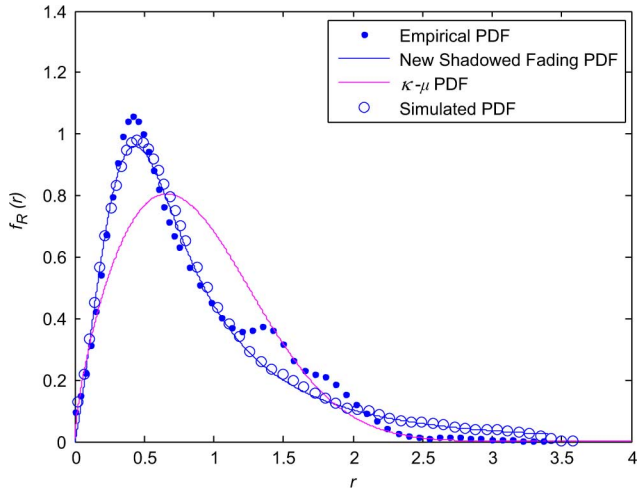

Fig. 7. Comparison of the NSF pdf and κ–μ pdf ($\kappa = 0.32$ and $\mu = 0.85$) fitted to the empirical pdf for the front-left-waist to right-wrist on-body link. Also shown is the simulated pdf obtained using the acceptance–rejection method [19].

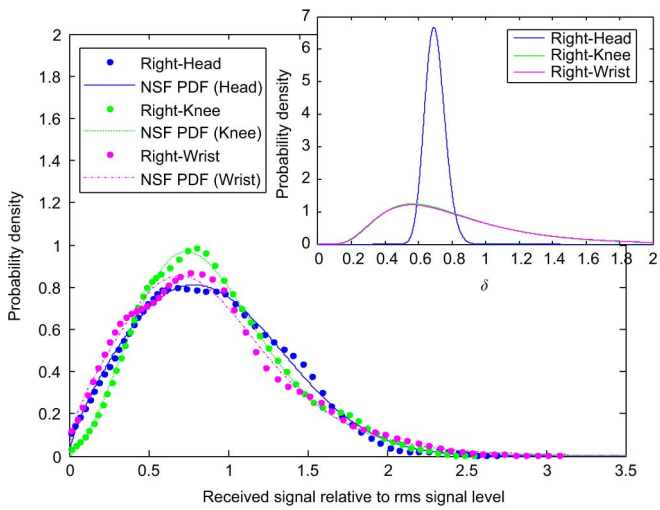

Fig. 8. NSF pdf fitted to the empirical pdf for each of the three on-body channels in the reverberation chamber. Shown inset is the estimated distribution of the shadowed resultant dominant component for each of the three links.

B. Off-Body

The results used to illustrate the utility of the proposed model for off-body channels were obtained from the field trials conducted in [5]. The experiments were performed in the same anechoic chamber described in Section IV-A. In this instance, the measurement hardware consisted of a NovaSource G6 RF source combined with a Hittite HMC-455LP3 low-noise amplifier configured to transmit a continuous wave signal with a power level of +22 dBm[2] at 2.42 GHz.

The transmit antenna used in this study was a flexible +6.2-dBi patch antenna [5, Fig. 1] designed to be resonant on the human body. The antenna had a −10-dB bandwidth of approximately 55 MHz (2.398–2.453 GHz) and was mounted with its ground plane parallel to the body surface of an adult male of height 1.95 m and mass 105 kg, at a height of 1.4 m. The antenna was positioned at the test subject's central chest region [Fig. 4(a)] and placed directly on his clothing using a small strip of Velcro® and without the use of a dielectric spacer. The receiver section of the measurement system consisted of an identical patch antenna connected to port 1 of a Rhode & Schwarz ZVB-8 VNA using a calibrated low-loss coaxial cable. The non-bodyworn antenna was mounted vertically on a nonconductive height adjustable stand at an elevation of 1.4 m above the floor level, corresponding to the height of the transmitter antenna. The VNA was then configured as a sampling receiver, recording the b_1 wave quantity incident on port 1 at a rate of 1 kHz for all experiments.

[2]The additional +22-dB transmit power used in this part of the study has been removed from the rms signal level presented in Table II so that the results from all three sections are referenced from a transmit power of 0 dBm.

TABLE II
ESTIMATED PARAMETERS FOR OFF-BODY AND BODY-TO-BODY CHANNELS USING NSF PDF

Off-Body					
Position	$\hat{\mu}$	$\hat{\sigma}$	$\hat{\alpha}$	$\hat{\beta}$	$\hat{r}$ (mV)
Rotation (1.5 m)	0.28	0.23	-0.47	2.54	1.14
Rotation (4 m)	0.56	0.22	-0.25	2.66	0.38
Mobile NLOS	0.85	0.64	-0.51	0.14	–
Body-to-Body					
Position	$\hat{\mu}$	$\hat{\sigma}$	$\hat{\alpha}$	$\hat{\beta}$	$\hat{r}$ (mV)
Rotation (1 m)	0.04	0.23	-2.85	2.96	1.14
Rotation (5 m)	0.44	0.22	0.13	2.65	0.19
Mobile NLOS	2.67	0.20	-0.27	0.48	–

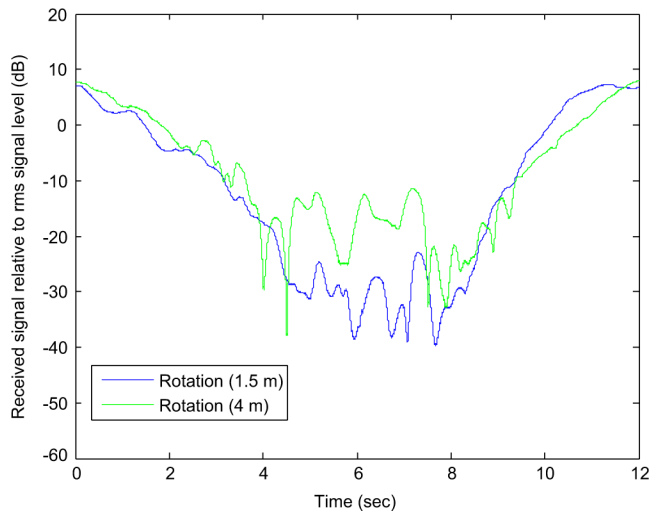

Fig. 9. Normalized received signal envelope for off-body channels while the user rotated at distances of 1.5 and 4 m from the receiver.

Two off-body channels which were anticipated to suffer greatly from body shadowing were investigated. The first scenario considered the rotation of a user in front of the receiver. In this set of measurements, the user rotated 360° (with his hands by his sides) in a counterclockwise direction from direct LOS between the transmit and receive antennas, through to the maximum shadowing condition where the user's body directly obstructed the main LOS path, before returning to LOS. Fig. 9 shows the normalized received signal envelopes as the user performed a rotation at a distance of 1.5 and 4 m from the receive antenna. As noted in [5], the general shape of the received signal envelope was observed to be comparable irrespective of distance.

Fig. 10 shows equation (10) fitted to the empirical probability density of the normalized signal envelope for the rotation data

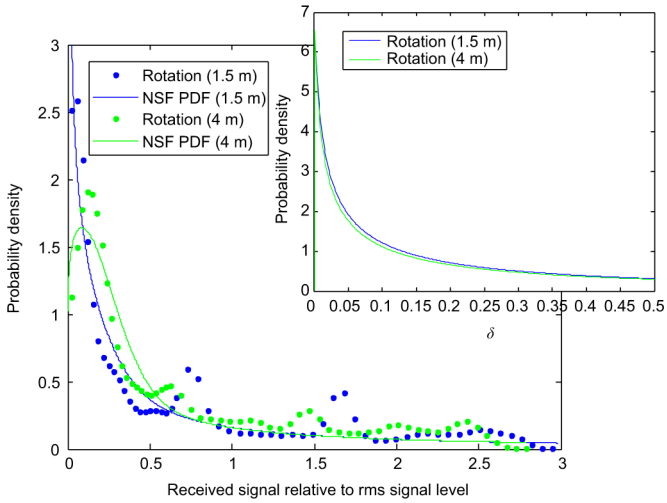

Fig. 10. NSF pdf fitted to the empirical pdf for off-body channels during user rotation in the anechoic chamber. Shown inset is the estimated distribution of the shadowed resultant dominant component for the two links.

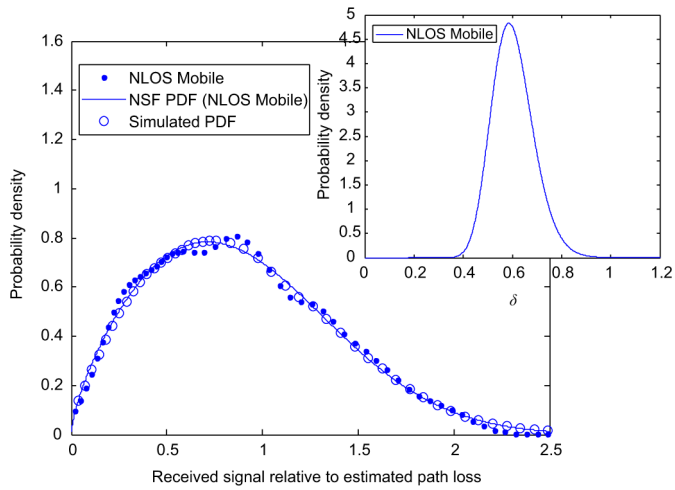

Fig. 11. NSF pdf and simulated pdf compared to the empirical pdf for off-body channel obtained for the user walking in NLOS in the anechoic chamber. Shown inset is the estimated distribution of the shadowed resultant dominant component for this link.

obtained at 1.5- and 4-m positions. The accompanying parameter estimates, obtained using the same process as outlined for the on-body analysis presented in Section IV-A, are given in Table II. As we can see, the NSF model presents a good fit to the experimental data. For the measurements made at a 1.5-m separation distance, the pdf of the normalized received signal indicates that this type of channel is subject to heavy body shadowing as the received signal is most frequently observed to be at low levels caused by the strong fading.

One of the most common scenarios that will be encountered in off-body communications will occur when the user simply walks so that their body obstructs the main LOS signal path [Fig. 1(b)]. To investigate this scenario, the user oriented themselves such that the chest-worn antenna was now in direct NLOS to the receive antenna. The user then walked the maximum permissible distance (6.5 m) away from the receive antenna. Fig. 11 shows the NSF and simulated pdfs compared with the empirical pdf obtained by removing the estimated path loss based on the elapsed time and average velocity using the model given in [5]. What is interesting here is that even under NLOS conditions and in the absence of multipath generated by the local environment a resultant dominant signal component still exists.

C. Body-to-Body

The bodyworn nodes used in this part of the validation study consisted of the body sensor node (BSN) platform developed by Imperial College London, London, U.K. [25] and presented in [14]. The transceiver section of the node utilized a Texas Instruments CC2420, which has a linear dynamic operating range of approximately 100 dB, a maximum transmit power of 0 dBm, and a receive sensitivity of −95 dBm. A transmitter node was configured to generate a continuous wave signal with a power level of 0 dBm at 2.45 GHz and a receiver node which was programmed to record the 8-bit received signal strength indicator (RSSI) obtained from the CC2420 every 16 ms. The BSN nodes were modified to replace the on-board chip antenna with the same flexible patch antenna used for the off-body channel measurements described in Section IV-B.

Unlike the on- and off-body measurements, the experiments conducted here were performed in an outdoor playing field at the Victoria Park recreational facilities in Belfast, U.K. The measurement environment consisted of a level grass play area which was bounded on three sides by trees and shrubbery and situated beside a soccer pitch adjoining on the remaining side. The area over which the measurements were performed was at least 50 m from each of these boundaries. The transmit and receive nodes were attached without the use of a dielectric spacer to the central chest region of two adult males of height 1.95 m and mass 105 kg (person A) and 1.82 m and mass 95 kg (person B), respectively, using a small strip of Velcro®. As shown in Fig. 4(b), the units were mounted directly on the test subject's clothing so that the ground plane of the antenna was parallel to the body surface.

The scenarios considered here were identical to those for the off-body channels. The first of these were rotational measurements where persons A and B stood facing one another with a separation distance of 1 m. Person A then performed a full 360° rotation, moving from direct LOS through to complete NLOS (180°) before returning to an LOS orientation. The estimated probability densities for the normalized signal envelopes recorded at the 1- and 5-m positions are shown in Fig. 12. The parameter estimates for the shadowed fading model pdf fitted to the data sets are given in Table II. As we can see by comparing Figs. 10 and 12, the characteristics of the shadow fading observed in this scenario are similar to the corresponding off-body channels.

For the mobile NLOS body-to-body measurements, person A started with their back toward person B at a separation distance of 1 m and walked in a straight line to a point 15 m away. As discussed in [14], due to the received signal regularly extending below the receive sensitivity of the body sensor nodes, only the first 6 s of person A walking in NLOS from person B were used in the analysis presented here. Fig. 13 shows the NSF and simulated pdfs compared with the empirical pdf obtained by removing the estimated path loss using the model given in [14]. Again, similar to the off-body scenario, even though one end of the link was shadowed by the user's body, a resultant

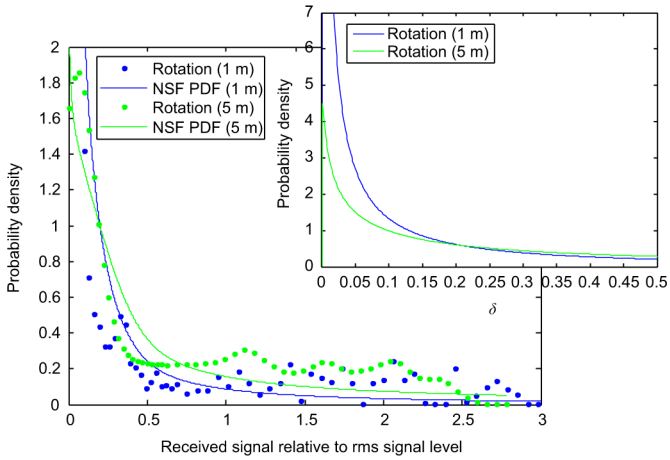

Fig. 12. NSF pdf fitted to the empirical pdf for body-to-body channels during user rotation in the outdoor environment. Shown inset is the estimated distribution of the shadowed resultant dominant component for the two links.

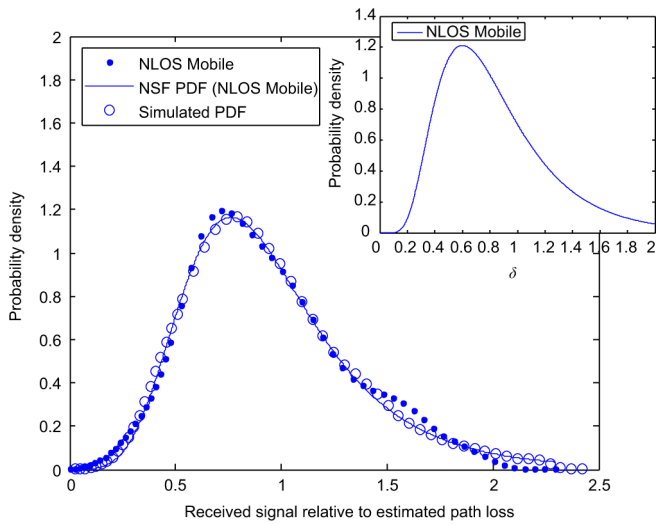

Fig. 13. NSF pdf and simulated pdf compared to the empirical pdf for body-to-body channel obtained for the user walking in NLOS in the outdoor environment. Shown inset is the estimated distribution of the shadowed resultant dominant component for this link.

dominant signal component was still observed to be present. It should be noted that the NSF model proposed here unifies the multipath and shadow fading observed over small distances in body-centric channels. Therefore, the parameter estimates given here can be used with the NSF pdf given in (10) in place of the separate model parameters for small body movements and body shadowing proposed in [5] and [14] to simulate off-body and body-to-body channels, respectively.

V. Conclusion

A novel statistical model for shadowing in body-centric communications channels has been presented. In this new model, the potential clustering of multipath components is considered alongside the presence of elective dominant signal components—a scenario which is similar to that observed in κ–μ fading. One notable difference between κ–μ fading and the model proposed here is that the resultant dominant component, formed by the phasor addition of the principal signal components, is subject to lognormal fading. This new model will find application well beyond the intended field of body-centric communications. It will be immediately useful in the study of land mobile satellite communications and other communications scenarios where the main signal paths may be subject to random shadowing. Additionally, the parameterization of this new model in terms of κ and μ will provide a useful addition to the growing family of statistics based on the existing κ–μ fading model.

Extensive validation of the proposed model has been achieved by considering three of the most commonly encountered body-centric networking applications, namely, on-body, off-body, and body-to-body communications. For each of the scenarios, the NSF model has been shown to provide an impressive fit to fading channels observed in the field. Finally, using the NSF pdf, simulation of the received signal levels likely to be obtained in body-centric communications channels has been achieved.

Acknowledgment

The author is extremely grateful to the reviewers of this manuscript and their invaluable comments which have helped to significantly improve the contribution of the work. The author would also like to thank Dr. G. A. Conway at Queen's University Belfast, Belfast, U.K., for designing the antennas used in this study. He is also extremely grateful to Prof. G. Z. Yang and Dr. B. P. L. Lo at Imperial College London, London, U.K., for providing the use of the body sensor nodes. Finally, he would also like to thank Dr. A. McKernan at ActivWireless Ltd., Belfast, U.K., for his assistance with the channel measurements conducted in this study.

References

[1] A. Alomainy, Y. Hao, A. Owadally, C. G. Parini, Y. Nechayev, C. C. Constantinou, and P. S. Hall, "Statistical analysis and performance evaluation for on-body radio propagation with microstrip patch antennas," *IEEE Trans. Antennas Propag.*, vol. 55, no. 1, pp. 245–248, Jan. 2007.

[2] P. V. Torre, L. Vallozzi, L. Jacobs, H. Rogier, M. Moeneclaey, and J. Verhaevert, "Characterization of measured indoor off-body MIMO channels with correlated fading, correlated shadowing and constant path loss," *IEEE Trans. Wireless Commun.*, vol. 11, no. 2, pp. 712–721, Feb. 2012.

[3] Y. Wang, I. B. Bonev, J. O. Nielsen, I. Z. Kovacs, and G. F. Pedersen, "Characterization of the indoor multiantenna body-to-body radio channel," *IEEE Trans. Antennas Propag.*, vol. 57, no. 4, pp. 972–979, Apr. 2009.

[4] R. Rosini, R. D'Errico, and R. Verdone, "Body-to-body communications: A measurement-based channel model at 2.45 GHz," in *Proc. IEEE 23rd Int. Symp. Pers. Indoor Mobile Radio Commun.*, Sep. 9–12, 2012, pp. 1763–1768.

[5] S. L. Cotton, A. McKernan, A. J. Ali, and W. G. Scanlon, "An experimental study on the impact of human body shadowing in off-body communications channels at 2.45 GHz," in *Proc. 5th Eur. Conf. Antennas Propag.*, Rome, Italy, Apr. 2011, pp. 3133–3137.

[6] S. Obayashi and J. Zander, "A body-shadowing model for indoor radio communication environments," *IEEE Trans. Antennas Propag.*, vol. 46, no. 6, pp. 920–927, Jun. 1998.

[7] D. B. Smith and D. Miniutti, "Cooperative selection combining in body area networks: Switching rates in gamma fading," *IEEE Wireless Commun. Lett.*, vol. 1, no. 4, pp. 284–287, Aug. 2012.

[8] C. Roblin and A. Sibille, "Modeling of the influence of body-worn antennas upon the path loss variability in UWB WBAN scenarios," in *Proc. URSI Gen. Assembly Sci. Symp.*, Istanbul, Turkey, Aug. 2011, DOI: 10.1109/URSIGASS.2011.6050534.

[9] L. Lingfeng, S. v. Roy, F. Quitin, P. D. Doncker, and C. Oestges, "Statistical characterization and modeling of Doppler spectrum in dynamic on-body channels," *IEEE Antennas Wireless Propag. Lett.*, vol. 12, pp. 186–189, 2013.
[10] S. L. Cotton and W. G. Scanlon, "Channel characterization for single and multiple antenna wearable systems used for indoor body-to-body communications," *IEEE Trans. Antennas Propag.*, vol. 57, Special Issue on Antennas & Propagation in Body-Centric Wireless Communications, no. 4, pp. 980–990, Apr. 2009.
[11] R. Rosini and R. D'Errico, "Comparing on-body dynamic channels for two antenna designs," in *Proc. Loughborough Antennas Propag. Conf.*, Nov. 2012, DOI: 10.1109/LAPC.2012.6402955.
[12] C. Oliveira and L. M. Correia, "A statistical model to characterize user influence in body area networks," in *Proc. IEEE Veh. Technol. Conf. Fall*, Sep. 2010, DOI: 10.1109/VETECF.2010.5594334.
[13] N. Chahat, G. Valerio, M. Zhadobov, and R. Sauleau, "On-body propagation at 60 GHz," *IEEE Trans. Antennas Propag.*, vol. 61, no. 4, pp. 1876–1888, Apr. 2013.
[14] S. L. Cotton, A. McKernan, and W. G. Scanlon, "Received signal characteristics of outdoor body-to-body communications channels at 2.45 GHz," in *Proc. Loughborough Antennas Propag. Conf.*, Nov. 2011, DOI: 10.1109/LAPC.2011.6114147.
[15] W. P. L. Cully, S. L. Cotton, W. G. Scanlon, and J. B. McQuiston, "Body shadowing mitigation using differentiated LOS/ NLOS channel models for RSSI-based Monte Carlo personnel localization," in *Proc. IEEE Wireless Commun. Netw. Conf.*, Paris, France, Apr. 2012, pp. 694–698.
[16] C. Loo, "A statistical model for a land mobile satellite link," *IEEE Trans. Veh. Technol.*, vol. 34, no. 3, pp. 122–127, Aug. 1985.
[17] A. Abdi, W. C. Lau, M.-S. Alouini, and M. Kaveh, "A new simple model for land mobile satellite channels: first- and second-order statistics," *IEEE Trans. Wireless Commun.*, vol. 2, no. 3, pp. 519–528, May 2003.
[18] M. D. Yacoub, "The κ–μ and the κ–μ distribution," *IEEE Antennas Propag. Mag.*, vol. 49, no. 1, pp. 68–81, Feb. 2007.
[19] W. L. Martinez and A. R. Martinez, *Computational Statistics with Matlab*, 2nd ed. London, U.K.: Chapman & Hall/CRC Press, 2008.
[20] S. L. Cotton and W. G. Scanlon, "An experimental investigation into the influence of user state and environment on fading characteristics in wireless body area networks at 2.45 GHz," *IEEE Trans. Wireless Commun.*, vol. 8, no. 1, pp. 6–12, Jan. 2009.
[21] G. A. Conway and W. G. Scanlon, "Antennas for over-body-surface communication at 2.45 GHz," *IEEE Trans. Antennas Propag.*, vol. 57, Special Issue on Antennas and Propagation on Body-Centric Wireless Communications, pp. 844–855, Apr. 2009.
[22] W. C. Jakes, *Microwave Mobile Communications*. New York, NY, USA: Wiley, 1974.
[23] M. Abramnowitz and I. A. Stegun, *Handbook of Mathematical Functions*. Washington, DC, USA: U.S. Dept. Commerce, Nat. Bureau Standards, 1972.
[24] S. L. Cotton, U. S. Dias, W. G. Scanlon, and M. D. Yacoub, "On the distribution of signal phase in body area networks," *IEEE Commun. Lett.*, vol. 14, no. 8, pp. 728–730, Aug. 2010.
[25] G. Z. Yang, *Body Sensor Networks*. New York, NY, USA: Springer-Verlag, 2006.

Simon L. Cotton (S'04–M'07) received the B.Eng. degree in electronics and software from the University of Ulster, Ulster, U.K., in 2004 and the Ph.D. degree in electrical and electronic engineering from the Queen's University of Belfast, Belfast, U.K., in 2007.

He is currently a Lecturer in Wireless Communications and an EPSRC/Royal Academy of Engineering Research Fellow at the Institute of Electronics, Communications and Information Technology (ECIT), Queen's University Belfast. He is also a Cofounder and the Chief Technology Officer at ActivWireless Ltd, Belfast, U.K. He has authored and coauthored over 60 publications in major IEEE/IET journals and refereed international conferences, two book chapters, and two patents. Among his research interests are cellular device-to-device, vehicular and body-centric communications. His other research interests include radio channel characterization and modeling and the simulation of wireless channels.

Dr. Cotton was awarded the H. A. Wheeler Prize, in July 2010, by the IEEE Antennas and Propagation Society for the best applications journal paper in the IEEE TRANSACTIONS ON ANTENNAS AND PROPAGATION during 2009. In July 2011, he was awarded the Sir George Macfarlane Award from the U.K. Royal Academy of Engineering in recognition of his technical and scientific attainment since graduating from his first degree in engineering.